Received 26 April 2016; | Revised 6 June 2016; | Accepted 6 June 2016

DOI: xxx/xxxx

RESEARCH ARTICLE

Analysis of NRD Guide Devices Using Rigorous Two-Dimensional Full-Vectorial FDTD Method

Tahir Bashir[1] | Keita Morimoto[1] | Akito Iguchi[1] | Yasuhide Tsuji*[1] | Tatsuya Kashiwa[2]

[1]Information and Electronic Engineering, Muroran Institute of Technology, Muroran, Japan

[2]Information and Communication Engineering, Kitami Institute of Technology, Kitami, Japan

Correspondence

*Yasuhide Tsuji, Information and Electronics Engineering, Muroran Institute of Technology, 27-1 Mizumoto-cho, Muroran, Hokkaido, 050-8585 Japan. Email: y-tsuji@mmm.muroran-it.ac.jp

Funding Information

This research was supported by the Japan Society for the Promotion of Science; JSPS KAKENHI Grant Number 21K04169

Summary

In this paper, rigorous two-dimensional full-vectorial finite difference time domain (2D-FVFDTD) method is developed for an efficient analysis of non-radiative dielectric waveguide (NRD guide) devices with three-dimensional structure. Convolutional perfectly matched layer (CPML) is employed as an absorbing boundary condition. Furthermore, we have established a rigorous formulation for estimating the modal power of each LSM_{01} and LSE_{01} mode. We confirmed the validity of the proposed method through the analysis of NRD crossing and T-branch guide devices. Excellent accuracy is achieved by the cross comparison of 2D-FVFDTD results with recently developed 2D-FVFEM.

KEYWORDS:

Non-radiative dielectric waveguide (NRD guide), Finite difference time domain (FDTD) method, Yee lattice

1 | INTRODUCTION

Millimeter waves or higher frequency electromagnetic waves attract a lot of attention for increasing communication capacity in 5G and beyond 5G. Non-radiative dielectric waveguide (NRD guide) is one of promising platforms of compact millimeter-wave circuits thanks to its non-radiative nature[1]. Although basic components based on NRD guide have been studied so far[1,2,3,4,5,6,7,8,9,10,11,12,13] advanced design of NRD devices using computer simulation based optimization techniques is desired to extremely enhance the performance of NRD circuits. To achieve efficient optimal design, high efficient numerical simulation techniques are indispensable.

Various kinds of electromagnetic simulation techniques have been developed so far. Among them, the finite element method (FEM)[14,15,16] and the finite-difference time-domain (FDTD)[17] method are probably most popular ones. Recently, we have developed two-dimensional full vectorial finite element method (2D-FVFEM)[18], which can efficiently analyze NRD guide devices without sacrificing numerical accuracy. The 2D-FVFEM has been successfully utilized for several optimal design of NRD guide devices including dielectric and magnetic materials[19,20,21,22,23,24,25]. On the other hand, time-domain simulation method is useful for analyzing broadband device properties. The 2D-FVFEM can be extended into a time domain analysis 2D-FV-FETD, but it could be more challenging as compared to 2D-FVFDTD. The FDTD scheme is explicit, whereas the 2D-FV-FETD scheme is implicit and requires a long computational time to solve the linear equations. The conventional 2D-FDTD solves only three field components in a two-dimensional waveguide or parallel plate dielectric waveguide with TE wave. It cannot be applied directly to the analysis of hybrid modes LSM_{01} and LSE_{01} in NRD guide. As a result, 3D-FDTD is widely used, but it requires a significant amount of computational time and simulation resources. Two-dimensional full vectorial FDTD (2D-FVFDTD), has been developed considering out-of-plane oscillation in 1990's[26,27]. In recent years, few 2D-FDTD methods for various applications

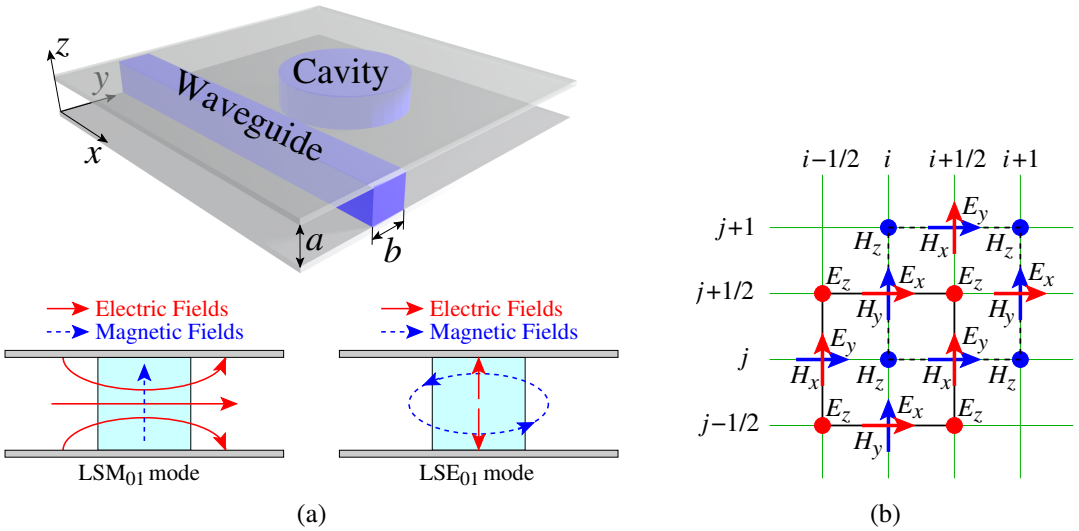

FIGURE 1 FDTD analysis of NRD guide device. (a) an image of NRD guide and supported modes, and (b) Yee lattice used in FDTD method.

have been proposed in the literature[28,29,30,31,32]. However, the applications of 2D-FVFDTD have been limited to the analysis of rectangular waveguides in microwave band so far.

Therefore, we develop 2D-FVFDTD method which can rigorously treat NRD guide structures with finite height. In terms of application, our 2D-FVFDTD method is developed for the analysis of millimeter-wave circuits based on NRD guides. From an algorithmic viewpoint, the proposed method can solve all six field components to treat hybrid modes, such as LSM_{01} and LSE_{01} modes where conventional 2D-FDTD fails to deal with these modes. We use analytic relation to the perpendicular direction of the parallel plates to reduce the spatial dimension to 2D. The forward and backward propagation in all three directions can be considered in our 2D-FVFDTD method. In our formulation, convolutional perfectly matched layer (CPML)[33] boundary condition developed in 2000's is employed. Furthermore, we establish a rigorous formulation for estimating the modal power of LSM_{01} and LSE_{01} modes contained in arbitrary propagation fields, which is validated by comparing the results of the proposed 2D-FVFDTD with recently developed 2D-FVFEM[18]. The accuracy of 2D-FVFEM has been verified by 3D- FVFEM[18,19,20,21]. In this method, the variations of electromagnetic fields are separated into parallel and vertical directions to metal plates and FDTD discretization is applied only to the field variation in the parallel direction. This approach can greatly reduce a computational effort because 3D analysis is not required without sacrificing rigorousness. This method can be used in 5G and beyond 5G to design the NRD waveguide devices with a similar structure in the THz band, but caution is required where conductor loss cannot be ignored. The validity of our approach is confirmed through numerical examples of crossing and T-branch NRD guides.

2 | FDTD FORMULATION FOR NRD GUIDE DEVICES

2.1 | Basic equation and FDTD discretization

We consider an NRD guide which supports two non-radiative modes of LSM_{01} and LSE_{01}[18], and propose 2D formulation of FDTD using Yee lattice, as shown in Fig. 1.

In NRD guide devices with no structural variation along the z-direction between parallel plates, the dependence of electric and magnetic fields on z can be expressed as follows:

$$E_x, E_y, H_z \propto \sin\left(\frac{\pi}{a}z\right), \qquad H_x, H_y, E_z \propto \cos\left(\frac{\pi}{a}z\right). \tag{1}$$

Then, Maxwell's equations can be written as follows:

$$\frac{\partial \phi_z}{\partial y} + s\left(\frac{\pi}{a}\right)\phi_y = sq\frac{\partial \psi_x}{\partial \tau} \qquad (\times f(z)) \tag{2}$$

$$-s\left(\frac{\pi}{a}\right)\phi_x - \frac{\partial \phi_z}{\partial x} = sq\frac{\partial \psi_y}{\partial \tau} \qquad (\times f(z)) \tag{3}$$

$$\frac{\partial \phi_y}{\partial x} - \frac{\partial \phi_x}{\partial y} = sq\frac{\partial \psi_z}{\partial \tau} \qquad (\times g(z)) \tag{4}$$

where $\tau = ct$, s, q, ϕ_ξ, and ψ_ξ ($\xi = x, y, z$) are defined as follows:

$$s = -1 \;\; q = 1 \;\; \phi_\xi = \sqrt{\varepsilon_0}\tilde{E}_\xi \;\; \psi_\xi = \sqrt{\mu_0}\tilde{H}_\xi \;\; f(z) = \cos(\pi z/a), \; g(z) = \sin(\pi z/a) \;\; \text{for Faraday's law,} \tag{5}$$

$$s = 1 \;\; q = \varepsilon_r \;\; \phi_\xi = \sqrt{\mu_0}\tilde{H}_w \;\; \psi_\xi = \sqrt{\varepsilon_0}\tilde{E}_\xi \;\; f(z) = \sin(\pi z/a), \; g(z) = \cos(\pi z/a) \;\; \text{for Ampére's law.} \tag{6}$$

In this formulation, ϕ_ξ and ψ_ξ do not depend on z, then, rigorous two-dimensional analysis becomes possible for NRD guide devices.

After discretization using Yee lattice, we can get the following FDTD update equations:

$$\psi^{(n_3)}_{x,i_2,j_1} = \psi^{(n_1)}_{x,i_2,j_1} + \frac{s\Delta\tau}{q_{i2,j1}}\left(\frac{\partial \phi^{(n_2)}_z}{\partial y} + \frac{\kappa_z}{s}\phi^{(n_2)}_y\right) \tag{7}$$

$$\frac{\partial \phi^{(n_2)}_z}{\partial y} = \frac{\phi^{(n_2)}_{z,i_2,j_2} - \phi^{(n_2)}_{z,i_2,j_0}}{\Delta y}, \;\; \phi^{(n_2)}_y = \phi^{(n_2)}_{y,i_2,j_1}$$

$$\psi^{(n_3)}_{y,i_1,j_2} = \psi^{(n_1)}_{y,i_1,j_2} + \frac{s\Delta\tau}{q_{i1,j2}}\left(-\frac{\kappa_z}{s}\phi^{(n_2)}_x - \frac{\partial \phi^{(n_2)}_z}{\partial x}\right) \tag{8}$$

$$\phi^{(n_2)}_x = \phi^{(n_2)}_{x,i_1,j_2}, \;\; \frac{\partial \phi^{(n_2)}_z}{\partial x} = \frac{\phi^{(n_2)}_{z,i_2,j_2} - \phi^{(n_2)}_{z,i_0,j_2}}{\Delta x}$$

$$\psi^{(n_3)}_{z,i_1,j_1} = \psi^{(n_1)}_{z,i_1,j_1} + \frac{s\Delta\tau}{q_{i1,j1}}\left(\frac{\partial \phi^{(n_2)}_y}{\partial x} - \frac{\partial \phi^{(n_2)}_x}{\partial y}\right) \tag{9}$$

$$\frac{\partial \phi^{(n_2)}_y}{\partial x} = \frac{\phi^{(n_2)}_{z,i_2,j_1} - \phi^{(n_2)}_{z,i_0,j_1}}{\Delta x}, \;\; \frac{\partial \phi^{(n_2)}_x}{\partial y} = \frac{\phi^{(n_2)}_{z,i_1,j_2} - \phi^{(n_2)}_{z,i_1,j_0}}{\Delta x}$$

where $\kappa_z = \pi/a$, and n_l, i_l, and j_l are respectively defined as: $m_l = m + (l-1)/2$ for Faraday's law, and $m_l = m + l/2$ for Ampére's law, where $m = n, i, j$.

2.2 | Convolutional Perfectly Matched Layer (CPML)

When using CPML[33], stretching coefficients of the stretched coordinate PML, s_ξ ($\xi = x, y, z$) are expressed as follows:

$$s_\xi = k_\xi + \frac{\sigma_\xi}{\alpha_\xi + j\omega}. \tag{10}$$

In the actual implementation, the frequency dependence of the stretching coefficients and relative permittivities are treated by using convolution integral. The final form of update equations of FDTD with CPML is expressed as follows:

$$\psi^{(n_3)}_{x,i_2,j_1} = C_{ax}\psi^{(n_1)}_{x,i_2,j_1} + C_{bx}\frac{s\Delta\tau}{q_{i2,j1}} \times \left(\frac{1}{k_y}\frac{\partial \phi^{(n_2)}_z}{\partial y} + \frac{1}{k_z}\frac{\kappa_z}{s}\phi^{(n_2)}_y + \Phi^{(n_2)}_{y,z} - \Phi^{(n_2)}_{z,y}\right) \tag{11}$$

$$\psi^{(n_3)}_{y,i_1,j_2} = C_{ay}\psi^{(n_1)}_{y,i_1,j_2} + C_{by}\frac{s\Delta\tau}{q_{i1,j2}} \times \left(-\frac{1}{k_z}\frac{\kappa_z}{s}\phi^{(n_2)}_x - \frac{1}{k_x}\frac{\partial \phi^{(n_2)}_z}{\partial x} + \Phi^{(n_2)}_{z,x} - \Phi^{(n_2)}_{x,z}\right) \tag{12}$$

$$\psi^{(n_3)}_{z,i_1,j_1} = C_{az}\psi^{(n_1)}_{z,i_1,j_1} + C_{bz}\frac{s\Delta\tau}{q_{i1,j1}} \times \left(\frac{1}{k_x}\frac{\partial \phi^{(n_2)}_y}{\partial x} - \frac{1}{k_y}\frac{\partial \phi^{(n_2)}_x}{\partial y} + \Phi^{(n_2)}_{x,y} - \Phi^{(n_2)}_{y,x}\right) \tag{13}$$

where $\Psi^{(n_2)}_{\xi,\eta}$, $C_{a\xi}$, and $C_{b\xi}$ are expressed as follows:

$$\Phi^{n2}_{\xi,\eta} = b_w \Phi^{n_0}_{\xi,\eta} + c_w \frac{\partial E^{(n_2)}_{\eta}}{\partial \xi}\Delta\tau, \;\; C_{a\xi} = 1, \;\; C_{b\xi} = \frac{\Delta\tau}{\varepsilon_r} \qquad \text{for Faraday's law} \tag{14}$$

$$\Phi^{n2}_{\xi,\eta} = b_w \Phi^{n_0}_{\xi,\eta} + c_w \frac{\partial H^{(n_2)}_{\eta}}{\partial \xi}\Delta\tau, \;\; C_{a\xi} = 1, \;\; C_{b\xi} = \Delta\tau \qquad \text{for Ampére's law} \tag{15}$$

where b_ξ and c_ξ are defined as follows:

$$b_\xi = \exp\left[-\left(\frac{\sigma_\xi}{k_\xi} + \alpha_\xi\right)\Delta\tau\right], \;\; c_\xi = \frac{\sigma_\xi}{k_\xi(\sigma_\xi + \alpha_\xi k_\xi)}(b_\xi - 1). \tag{16}$$

2.3 | Evaluation of frequency spectrum using Fourier transform

In order to evaluate frequency characteristics of transmission and reflection power, we have to calculate Fourier transform of time-dependent modal amplitude at reference plane. The modal amplitude of reference plane is calculated by the following overlap integral with each modal field at each time step:

$$a_{\mathrm{LSM}_{01}} = \int_\Gamma \frac{1}{\varepsilon_r}\tilde{H}_z^{\mathrm{LSM}_{01}}\tilde{H}_z d\Gamma \qquad \text{for } \mathrm{LSM}_{01} \text{ mode} \tag{17}$$

$$a_{\mathrm{LSE}_{01}} = \int_\Gamma \tilde{E}_z^{\mathrm{LSE}_{01}}\tilde{E}_z d\Gamma \qquad \text{for } \mathrm{LSE}_{01} \text{ mode} \tag{18}$$

After calculating time evolutions of modal amplitudes and their Fourier transforms, normalized power of target mode (MODE : LSM_{01} or LSE_{01}) is calculated as follows:

$$P_{\mathrm{MODE}} = \frac{\beta_{\mathrm{LSM}_{01}}\left\{(\pi/a)^2 + \beta^2_{\mathrm{MODE}}\right\}}{\beta_{\mathrm{MODE}}\left\{(\pi/a)^2 + \beta^2_{\mathrm{LSM}_{01}}\right\}}\frac{\left|A_{\mathrm{MODE}}\right|^2}{\left|A^{(\mathrm{in})}_{\mathrm{LSM}_{01}}\right|^2} \tag{19}$$

where A_{MODE} and $A^{(\mathrm{in})}_{\mathrm{LSM}_{01}}$ are Fourier transforms of a_{MODE} and the modal amplitude of the incidence wave, respectively.

3 | NUMERICAL EXAMPLES

In order to verify the accuracy of the proposed 2D-FVFDTD method, we consider two types of NRD guide components. The separation between metal plates of NRD guide is assumed to be $a = 2.25$ mm and width of the dielectric strip between these plates is $b = 2$ mm with relative permittivity $\varepsilon_r = 2.2$. The surrounding region is assumed to be air with relative permittivity $\varepsilon_{\mathrm{air}} = 1$. Furthermore, LSM_{01} Gaussian pulse with center frequency of 60 GHz is considered for excitation at input port 1.

3.1 | Crossing Waveguide

First, we consider an NRD crossing waveguide whose geometrical parameters are as follow: $W_x = 60$ mm, $W_y = 40$ mm, $l_1 = 5$ mm, $l_2 = 24$ mm, and $d_{\mathrm{PML}} = 10$ mm as shown in Fig. 2. The computational region is discretized using Yee lattice with size of $\Delta x = \Delta y = 0.05$ mm and time step $\Delta t = \Delta x/2c$ ($< \Delta t_{\mathrm{CFL}}$) where c is the light velocity and $\Delta t_{\mathrm{CFL}} = \Delta x/(\sqrt{2}c)$ is the upper limit for the time step under the CFL condition. The time step size is $\Delta t = 83.4$ fs and the total number of time steps is 80,000 for the developed 2D-FVFDTD. In this numerical example, Gaussian time pulse is excited at $x = 15$ mm and time evolution of modal amplitudes are observed at four reference planes, $\Gamma_{1\sim4}$, in port $1 \sim 4$ as shown in Fig. 2. Since the excitation is symmetrically given to $\pm x$-directions, the first peak in the port 1 corresponds to the incident pulse and the following wave corresponds to reflected wave. The propagation fields in the crossing waveguide at some different time steps are shown in Fig. 2. Figure 3 shows the frequency characteristics of the crossing waveguide calculated by the proposed method and the 2D-FVFEM whose validity is confirmed by comparing with 3D-FEM [18]. In Fig. 3, LSM_{01} mode of 2D-FVFDTD is slightly off with 2D-FVFEM due to strong frequency dependence around 60 GHz as compare to LSE_{01} mode. The accuracy may degrade more at lower frequencies due to strong modal dispersion near the cut-off frequency. Although LSM_{01} mode is slightly off but both results are in good agreement and the effectiveness and usefulness of the proposed method are confirmed.

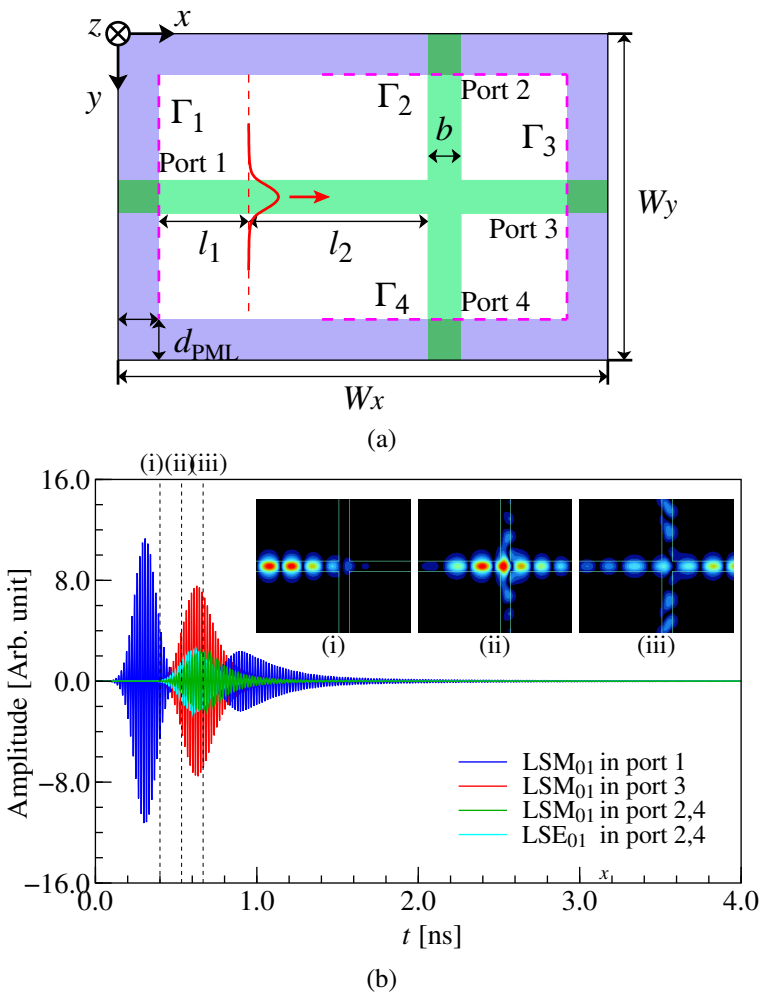

FIGURE 2 2D-FVFDTD analysis of NRD crossing waveguide. (a) Schematic diagram, (b) Time evolutions of modal amplitudes at the reference plane 1 ($x = 10$ mm), reference plane 2 ($y = 10$ mm), reference plane 3 ($y = 30$ mm) and reference plane 4 ($y = 30$ mm). Time evolutions of both LSM_{01} and LSE_{01} modes are evaluated.

3.2 | T-branch Waveguide

As an another numerical example, we consider a T-branch waveguide as shown in Fig. 4. The analysis model is the same as the previous one except that port 3 is removed. The time evolutions at reference planes and propagating fields at three different time steps are shown in Fig. 4. Figure 5 shows the frequency characteristics of the T-branch waveguide calculated by the proposed method and the 2D-FVFEM. We can see that both results are in good agreement in this numerical example too. If 3D analysis is necessary in the numerical examples considered here, 45 times more unknowns are required than with our 2D-FVFDTD method, because the parallel plate separation is 2.25 mm and the Yee lattice size is 0.05 mm in each direction is used. As a result, when compared to the 3D-FDTD approach, both computing time and memory requirements can be reduced by a factor of 45. The computational cost of the proposed 2D-FVFDTD method and comparison with other simulation methods is shown in Table 1. The 2D-FVFDTD analysis used only 7.32 min. with 1.1 GB of memory for computation at Intel(R) Xeon(R) Gold 6242 CPU @ 2.80 GHz. We can see how efficient our originally developed 2D algorithms are for 3D structures.

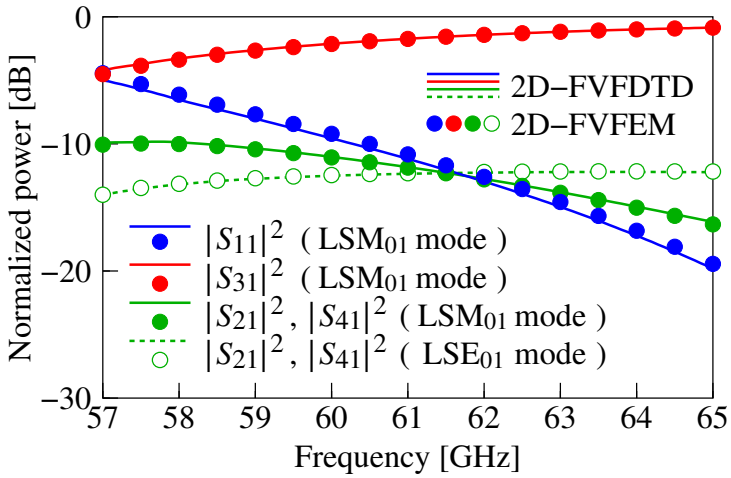

FIGURE 3 Frequency characteristics of crossing waveguide.

TABLE 1 Comparison of computational cost between different simulation methods

Methods	Time [min.]	Memory [GB]
2D-FVFDTD	7.32	1.1
3D-FVFDTD	329.4	49.5
2D-FVFEM	2.24	0.2
3D-FVFEM	628.3	78.8

The above times are for calculating 80,000 time steps in FDTD and for 100 frequencies in FEM.

4 | CONCLUSION

In this paper, we proposed 2D-FVFDTD method for efficient analysis of NRD guide devices. We confirmed the validity of the proposed method through the frequency characteristics analysis of two NRD guide components. Efficient time domain numerical simulation techniques are desired, especially for optimal design of NRD guide devices with broad operation bandwidth and filtering devices because frequency characteristics can be obtained by single FDTD analysis, while in frequency domain analysis, responses at a lot of discrete frequency have to be calculated. We are considering to develop optimal design algorithm for high performance NRD guide devices utilizing the proposed method. In the future, we intend to extend the modeling beyond 5G to the THz range. In addition, we will extend proposed method with magnetic materials to efficiently simulate the non-reciprocal devices such as NRD circulator and isolators.

ACKNOWLEDGMENTS

This work was supported by JSPS (Japan) KAKENHI Grant Number 21K04169 and 22K04234.

Conflict of interest

The authors declare no potential conflict of interests.

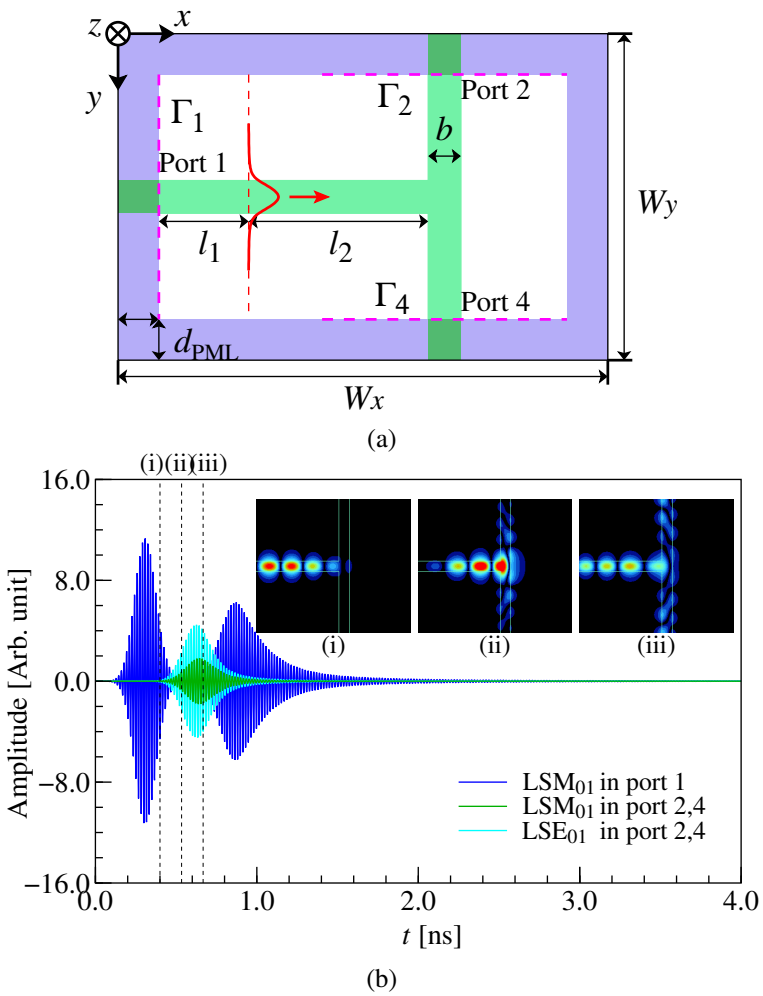

FIGURE 4 2D-FVFDTD analysis of NRD T-branch waveguide. (a) Schematic diagram, (b) Time evolutions of modal amplitudes at the reference plane 1 ($x = 10$ mm), reference plane 2 ($y = 10$ mm), and reference plane 4 ($y = 30$ mm). Time evolutions of both LSM_{01} and LSE_{01} modes are evaluated.

References

[1] Yoneyama T, Nishida S. Nonradiative Dielectric Waveguide for Millimeter-Wave Integrated Circuits. *IEEE Transactions on Microwave Theory and Techniques* 1981; 29(11): 1188-1192. doi: 10.1109/TMTT.1981.1130529

[2] Yoneyama T. Recent development in NRD-guide technology. *In Annales des télécommunications* 1992; 47(11): 508-514. doi: 10.1007/BF02998313

[3] Maamria K, Wagatsuma T, Yoneyama T. Leaky NRD guide as a feeder for microwave planar antennas. *IEEE Transactions on Antennas and Propagation* 1993; 41(12): 1680-1686. doi: 10.1109/8.273312

[4] Wu K. A combined efficient approach for analysis of nonradiative dielectric (NRD) waveguide components. *IEEE Transactions on Microwave Theory and Techniques* 1994; 42(4): 672-677. doi: 10.1109/22.285075

[5] Huang J, Wu K, Kuroki F, Yoneyama T. Computer-aided design and optimization of NRD-guide mode suppressors. *IEEE Transactions on Microwave Theory and Techniques* 1996; 44(6): 905-910. doi: 10.1109/22.506450

[6] Wu K, Han L. Hybrid integration technology of planar circuits and NRD-guide for cost-effective microwave and millimeter-wave applications. *IEEE Transactions on Microwave Theory and Techniques* 1997; 45(6): 946-954. doi: 10.1109/22.588607

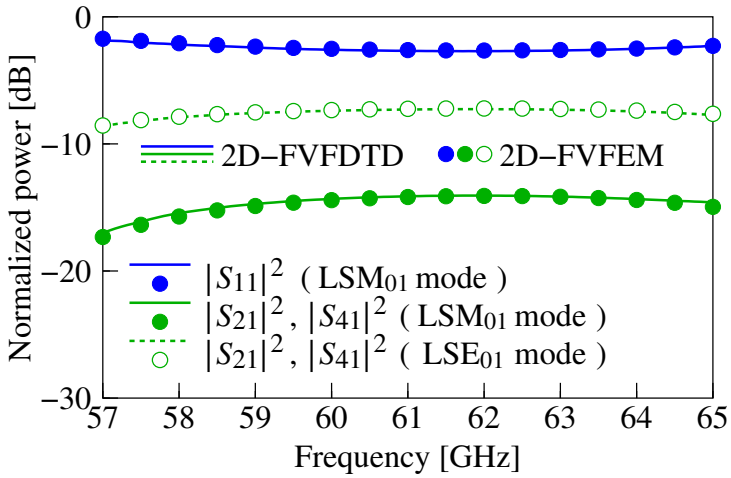

FIGURE 5 Frequency characteristics of T-branch waveguide.

[7] Dallaire J, Wu K. Complete characterization of transmission losses in generalized nonradiative dielectric (NRD) waveguide. *IEEE Transactions on Microwave Theory and Techniques* 2000; 48(1): 121-125. doi: 10.1109/22.817480

[8] Boone F, Wu K. Mode conversion and design consideration of integrated nonradiative dielectric (NRD) components and discontinuities. *IEEE Transactions on Microwave Theory and Techniques* 2000; 48(4): 482-492. doi: 10.1109/22.842018

[9] Kuroki F, Wada K, Yoneyama T. Low-loss and small-sized NRD guide ring resonators and their application to channel dropping filter at 60 GHz. *IEEE Transactions on Electronics* 2003; E86-C(8): 1601-1606.

[10] Lee J, Lee J, Im C, Kim H, Choi K, Jung HK. Selection of proper modes of an NRD guide using a perturbing boundary. *IEEE Transactions on Magnetics* 2003; 39(3): 1246-1249. doi: 10.1109/TMAG.2003.810339

[11] Schmid U, Menzel W. A 24 GHz microstrip antenna array with a non-radiative dielectric waveguide (NRD-guide) feeding network. *11th International Symposium on Antenna Technology and Applied Electromagnetics [ANTEM 2005]* 2005: 1-4. doi: 10.1109/ANTEM.2005.7852158

[12] Li D, Cassivi Y, Yang P, Wu K. Analysis and design of bridged NRD-guide coupler for millimeter-wave applications. *IEEE Transactions on Microwave Theory and Techniques* 2005; 53(8): 2546-2551. doi: 10.1109/TMTT.2005.852764

[13] Kuroki F, Kimura M, Yoneyama T. A Transition between NRD Guide and Microstrip Line at 60 GHz. *IEEE Transactions on Electronics* 2005; E88-C(10): 1968-1972. doi: 10.1093/ietele/e88-c.10.1968

[14] Rahman B, Fernandez F, Davies J. Review of finite element methods for microwave and optical waveguides. *Proceedings of the IEEE* 1991; 79(10): 1442-1448. doi: 10.1109/5.104219

[15] Jin JM. The Finite Element Method in Electromagnetics, 3rd Edition. *Wiley-IEEE Press* 2014.

[16] Tsuji Y, Koshiba M. Finite element method using port truncation by perfectly matched layer boundary conditions for optical waveguide discontinuity problems. *Journal of Lightwave Technology* 2002; 20(3): 463-468. doi: 10.1109/50.988995

[17] Taflove A, Hagness SC. Computational electromagnetics – the finite difference time-domain method. *Artech House* 2005.

[18] Tsuji Y, Morimoto K, Iguchi A, Kashiwa T, Nishiwaki S. Two-Dimensional Full-Vectorial Finite Element Analysis of NRD Guide Devices. *IEEE Microwave and Wireless Components Letters* 2021; 31(4): 345-348. doi: 10.1109/LMWC.2021.3060179

[19] Bashir T, Morimoto K, Iguchi A, Tsuji Y, Kashiwa T, Nishiwaki S. Optimal Design of NRD Guide Devices Using 2D Full-Vectorial Finite Element Method. *IEICE Electronics Express* 2021; 18(15): 1-4. doi: 10.1587/elex.18.20210243

[20] Bashir T, Morimoto K, Iguchi A, Tsuji Y, Kashiwa T. Optimal Design of 90 °-Bend in NRD Guide Using DBS Algorithm and 2D-FVFEM. *2021 IEEE International Symposium on Antennas and Propagation and USNC-URSI Radio Science Meeting (APS/URSI)* 2021: 1643-1644. doi: 10.1109/APS/URSI47566.2021.9704465

[21] Bashir T, Morimoto K, Iguchi A, Tsuji Y, Kashiwa T, Nishiwaki S. Optimal design of broadband non-radiative dielectric guide devices using binary genetic algorithm and 2D-FVFEM. *International Journal of Numerical Modelling: Electronic Networks, Devices and Fields* 2022. doi: 10.1002/jnm.2984

[22] Kashiwa T, Tsuji Y. Topology Optimization of NRD Waveguide for Millimeter-wave Integrated Circuits. *IEICE Trans. Electronics. (Japanese Edition)* 2022; J105-C(3). doi: 10.14923/transcomj.2021JBI0002

[23] Hieda N, Morimoto K, Iguchi A, Tsuji Y, Kashiwa T. Topology Optimal Design of NRD Guide Devices Using Function Expansion Method and Evolutionary Approaches. *IEICE Tansactions on Electronics, submitted for publication* 2022.

[24] Bashir T, Morimoto K, Iguchi A, Tsuji Y, Kashiwa T. Mosaic Based Optimization of NRD Guide Devices Using Binary Evolutionary Approaches and 2D-FVFEM. *IEEE Access* 2022; 10: 60682-60695. doi: 10.1109/ACCESS.2022.3180732

[25] Bashir T, Morimoto K, Iguchi A, Tsuji Y, Kashiwa T. Optimal design of NRD isolator using Ni-Zn ferrite post for millimeter-wave integrated circuit applications. *2022 Asia-Pacific Microwave Conference (APMC)* 2022.

[26] Mroczkowski C, Gwarek WK. Microwave Circuits Described by Two-Dimensional Vector Wave Equation and their Analysis by FD-TD Method. *1991 21st European Microwave Conference* 1991; 1: 866-871. doi: 10.1109/EUMA.1991.336411

[27] Gwarek W, Morawski T, Mroczkowski C. Application of the FD-TD method to the analysis of circuits described by the two-dimensional vector wave equation. *IEEE Transactions on Microwave Theory and Techniques* 1993; 41(2): 311-317. doi: 10.1109/22.216473

[28] Yechou L, Tribak A, Kacim M, Serroukh A, Tarhzaz J. Waveguide High-pass filter Design and 2D-FDTD Analysis method. *Revue Méditerranéenne des Télécommunications* 2019; 9(1): 1-14.

[29] Ramzi G, Hichem T, Ali G. 2-D FDFD method analysis to NRD-guide bandpass filter design. *2014 1st International Conference on Advanced Technologies for Signal and Image Processing (ATSIP)* 2014: 560-563. doi: 10.1109/ATSIP.2014.6834676

[30] Luo S, Chen Z. A New 2D FDTD Method for Solving 3D Guided-wave Structures. *2006 IEEE MTT-S International Microwave Symposium Digest* 2006: 1473-1476. doi: 10.1109/MWSYM.2006.249569

[31] Mehennaoui N, Merzouki A, Slimani D. 2D-FDTD-UPML simulation of wave propagation on dispersive media. *2015 3rd International Conference on Control, Engineering & Information Technology (CEIT)* 2015: 1-5. doi: 10.1109/CEIT.2015.7233034

[32] Shamy RSE, Swillam M, Obayya S. Full 3D electromagnetic wave analysis using 2D simulation. *2017 International Applied Computational Electromagnetics Society Symposium - Italy (ACES)* 2017: 1-2. doi: 10.23919/ROPACES.2017.7916021

[33] Roden JA, Gedney SD. Convolutional PML (CPML): an efficient FDTD implementation of the CFS-PML for arbitrary media. *Microwave and Optical Technology Letters* 2000; 27(5): 334-339. doi: 10.1002/1098-2760(20001205)27:5<334::AID-MOP14>3.0.CO;2-A

How to cite this article: T. Bashir, K. Morimoto, A. Iguchi, Y. Tsuji, and T. Kashiwa (2022), Analysis of NRD Guide Devices Using Rigorous Two-Dimensional Full-Vectorial FDTD Method, *Microw and Optical Technology Letters*, *2022;00:1–6*.